Developmental Cell *10*, 587–600, May, 2006 ©2006 Elsevier Inc. DOI 10.1016/j.devcel.2006.04.012

The Peroxisomal Membrane Protein Inp2p Is the Peroxisome-Specific Receptor for the Myosin V Motor Myo2p of *Saccharomyces cerevisiae*

Andrei Fagarasanu,[1] Monica Fagarasanu,[1] Gary A. Eitzen,[1] John D. Aitchison,[2] and Richard A. Rachubinski[1,*]

[1] Department of Cell Biology
University of Alberta
Edmonton, Alberta T6G 2H7
Canada

[2] Institute for Systems Biology
Seattle, Washington 98103

Summary

The faithful inheritance of organelles by daughter cells is essential to maintain the benefits afforded to eukaryotic cells by compartmentalization of biochemical functions. In *Saccharomyces cerevisiae*, the class V myosin, Myo2p, is involved in transporting different organelles, including the peroxisome, along actin cables to the bud. We identified Inp2p as the peroxisome-specific receptor for Myo2p. Cells lacking Inp2p fail to partition peroxisomes to the bud but are unaffected in the inheritance of other organelles. Inp2p is a peroxisomal membrane protein, preferentially enriched in peroxisomes delivered to the bud. Inp2p interacts directly with the globular tail of Myo2p. Cells overproducing Inp2p often transfer their entire populations of peroxisomes to buds. The levels of Inp2p oscillate with the cell cycle. Organelle-specific receptors like Inp2p explain how a single motor can move different organelles in distinct and specific patterns. To our knowledge, Inp2p is the first peroxisomal protein implicated in the vectorial movement of peroxisomes.

Introduction

Organelles are faithfully inherited by daughter cells at cell division. To ensure the accuracy of this process, organelles use highly regulated and coordinated strategies for partitioning that involve movement along microtubules or actin driven by molecular motors (Warren and Wickner, 1996). In most eukaryotic cells, the long-range movements of organelles occur along microtubules, while actin-based motility is favored for short-range transport. Movement along actin is performed by actin-based myosin motors, particularly members of the class V myosins.

Class V myosins are present in most eukaryotic cells and are ideally suited for organelle trafficking. The divergent carboxy-terminal tail domains of these unconventional myosins contain the information necessary for their targeting to specific intracellular compartments (Seabra and Coudrier, 2004). Class V myosins function in the distribution of cellular components by interacting with their cargoes and transporting them via their amino-terminal motor domain along actin tracks. Many myosin V cargoes have been identified in different cell types and within a single cell type. Thus, class V myosins participate in a broad range of cellular functions, and a given class V myosin can serve multiple functions (Reck-Peterson et al., 2000; Wu et al., 2000).

The budding yeast *Saccharomyces cerevisiae* has proven to be an excellent model system with which to study organelle movement and inheritance. In contrast to cells that divide by fission, *S. cerevisiae* must actively and vectorially deliver its organelles to the growing bud (Rossanese and Glick, 2001). To achieve this, cells strategically localize their formins, Bni1p and Bnr1p, at the nascent bud site and bud neck (Pruyne et al. 2004). These proteins are specially designed to assemble actin filaments while holding onto their growing barbed ends (Bretscher, 2003). The resulting polarized array of actin cables is used as tracks by class V myosins to transport organelles to the daughter cell, thereby ensuring their proper segregation.

Myo2p and Myo4p are the myosin V actin-based motors responsible for the partitioning of intracellular compartments in budding yeast (for reviews see Bretscher, 2003; Pruyne et al., 2004). Myo4p is not essential and is involved in the inheritance of cortical ER (Estrada et al., 2003) and in the transport of several mRNAs (Shepard et al., 2003). In contrast, Myo2p is an essential protein that moves a series of cargoes, including secretory vesicles (Govindan et al., 1995; Schott et al., 1999), the vacuole (Hill et al., 1996; Catlett et al., 2000), late compartments of the Golgi (Rossanese et al., 2001), and peroxisomes (Hoepfner et al., 2001). Myo2p is also required for orientation of the mitotic spindle (Yin et al., 2000) and appears to play a role in mitochondrial inheritance (Boldogh et al., 2004; Itoh et al., 2004).

Interestingly, Myo2p-dependent delivery of the vacuole and secretory vesicles can be dissected in the Myo2p tail (Schott et al., 1999; Catlett et al., 2000). Also, the time of movement and destination of each Myo2p cargo are overlapping but not identical (Weisman, 2003). It has thus been proposed that each organelle has its own Myo2p-specific receptor that binds to different regions in the Myo2p tail. Given the large diversity of myosin ligands and the deleterious effect of competition among them, these organelle-specific factors must be strictly regulated by the cell to act in coordination with cell cycle events. One example of this strict regulation is provided by vacuole inheritance. The levels of Vac17p, the vacuole-specific receptor for Myo2p, increase at a specific time in the cell cycle (Tang et al., 2003). The newly synthesized Vac17p in the mother cell attaches to the vacuole membrane, providing a link between Vac8p and Myo2p (Ishikawa et al., 2003; Tang et al., 2003). This results in the delivery of the attached vacuole membrane along actin tracks to the bud. There, Vac17p is degraded in a PEST-dependent manner, releasing Myo2p to perform other functions and, at the same time, ensuring the vectorial transport of the vacuole, which is thus delivered to its specific destination (Bretscher, 2003; Tang et al., 2003). To date, Vac17p represents the only identified receptor for Myo2p of a membrane-bound organelle.

*Correspondence: rick.rachubinski@ualberta.ca

Apart from its role in carrying membrane-bound organelles, Myo2p is also involved in orienting the intranuclear mitotic spindle along the mother-bud axis (Bretscher, 2003). Myo2p does this by associating with the plus ends of cytoplasmic microtubules and actively transporting them into the bud. The link between Myo2p and the ends of microtubules is provided by the Kar9p-Bim1p complex (Lee et al., 2000; Yin et al., 2000). Interestingly, Kar9p decorates only those cytoplasmic microtubules that emanate from the spindle pole body destined for the daughter cell (Liakopoulos et al., 2003). This ensures that only one spindle pole body is delivered to the bud and results in the proper alignment of the mitotic spindle with the predetermined cell division axis (Liakopoulos et al., 2003).

Peroxisome movement in budding yeast is also dependent on Myo2p (Hoepfner et al., 2001). During cell division, about half of peroxisomes are delivered to the bud, while the remaining half is retained at the mother cell cortex (Hoepfner et al., 2001; Fagarasanu et al., 2005). The recently identified peroxisomal protein Inp1p is essential for the retention of a subset of peroxisomes at the cell periphery (Fagarasanu et al., 2005). Since Inp1p has an intrinsic affinity for the cell cortex, it may provide the link between peroxisomes and an as of yet unidentified cortical anchor (Fagarasanu et al., 2005). However, how peroxisomes capture Myo2p for their transport to the bud remains unknown. Here we identify and characterize Inp2p as a novel peroxisomal membrane protein that functions as the peroxisome-specific receptor for Myo2p.

Results

Peroxisome Dynamics in Wild-Type *S. cerevisiae* Cells

We use three-dimensional time-lapse (4D) confocal video microscopy (Hammond and Glick, 2000) of *S. cerevisiae* cells expressing a genomically integrated chimeric gene, *POT1-GFP*, encoding peroxisomal thiolase tagged at its carboxyl terminus with GFP (Pot1p-GFP) to examine the dynamics of peroxisomes (Fagarasanu et al., 2005). In wild-type cells, most peroxisomes are immobile at the cell periphery (Figures 1A and 1B; Supplemental Movies S1 and S2). During bud growth, peroxisomes are recruited one by one from these static positions and transported toward the bud (Figure 1C; Movie S3). The velocities of these mobile peroxisomes vary, with a maximal observed velocity of approximately 0.45μm/s (Figure 1D; Figure S1). Interestingly, peroxisomes in the bud concentrate at sites of polarized cell growth, initially clustering at the bud tip. During cytokinesis, subsets of peroxisomes in the bud and in the mother cell relocate to the bud-neck region, while the remaining peroxisomes remain immobile at the bud and mother cell cortices (Figure 1A; Movie S1).

Identification of Inp2p

The partitioning of peroxisomes to buds has been shown to be dependent on Myo2p (Hoepfner et al., 2001). The interaction of Myo2p with organelles is modulated by receptors that recognize Myo2p and are postulated to be specific for individual types of organelles. We initially set out to identify the peroxisome-specific receptor for Myo2p by screening haploid yeast strains deleted for nonessential genes and that could exhibit compromised peroxisome inheritance. To reduce the overall number of strains to be screened, we stipulated that the peroxisome-specific receptor for Myo2p should satisfy two criteria. First, such a receptor must be localized to peroxisomes. In addition to the known peroxisomal proteins, we were interested in proteins exhibiting a "punctate composite" distribution as defined in the study reporting a global analysis of protein localization in *S. cerevisiae* (Huh et al., 2003). We also focused on proteins predicted to contain coiled-coil domains, since these domains have been found in other proteins that directly interact with the globular tail of class V myosins (Nagashima et al., 2002; Estrada et al., 2003; Ishikawa et al., 2003; Itoh et al., 2004).

To identify strains defective in peroxisome inheritance, cells of individual deletion strains expressing *POT1-GFP* were scored using a stringent all-or-none criterion for the presence of peroxisomal fluorescence within buds (see Supplemental Experimental Procedures). Analysis of approximately 250 deletion mutant strains yielded one strain that was dramatically affected in peroxisome inheritance. This strain was deleted for the open reading frame *YMR163c*, encoding a protein of unknown function, Ymr163p (*Saccharomyces* Genome Database, http://www.yeastgenome.org/). Ymr163p satisfies both of our a priori selection criteria for a peroxisomal receptor for Myo2p. Its GFP chimera yields a "punctate composite" fluorescence pattern (Huh et al., 2003). Ymr163p is predicted to be 705 amino acids in length and to have two coiled-coiled domains (amino acids 477–504 and 618–646). Because of its role in peroxisome inheritance (see below), we have designated *YMR163c* as *INP2* for inheritance of peroxisomes gene 2 and its encoded protein as Inp2p.

Cells Lacking Inp2p Exhibit a Specific Impairment in Peroxisome Inheritance

Budded cells of the *inp2Δ* strain displayed an increase in the percentage of buds devoid of peroxisomes as compared to wild-type cells (Figure 2A). Quantification showed that when the bud volume reached 0%–12% of the mother cell volume (Category I), only 3.7% of the buds of the *inp2Δ* strain contained at least one peroxisome. In contrast, 90% of Category I buds of wild-type cells had peroxisomes. Overall, *inp2Δ* cells exhibited less buds containing at least one peroxisome than wild-type cells at all bud sizes. For *inp2Δ* cells, only 21%, 26%, and 30% of buds of Categories II, III, and IV, respectively, displayed peroxisomal fluorescence, while essentially 100% of wild-type buds in each of these categories contained peroxisomes (Figure 2A). In addition, we observed that whereas wild-type cells contained a fairly equal number of peroxisomes per cell, *inp2Δ* cells displayed heterogeneity in their number of peroxisomes. Some *inp2Δ* cells exhibited increased numbers of peroxisomes, while others exhibited few or even no peroxisomes.

The impairment in peroxisome segregation observed in cells lacking Inp2p could be due theoretically to generalized defects in cell polarity or acto-myosin function. To test if Inp2p is required specifically for peroxisome inheritance, we examined the partitioning of other

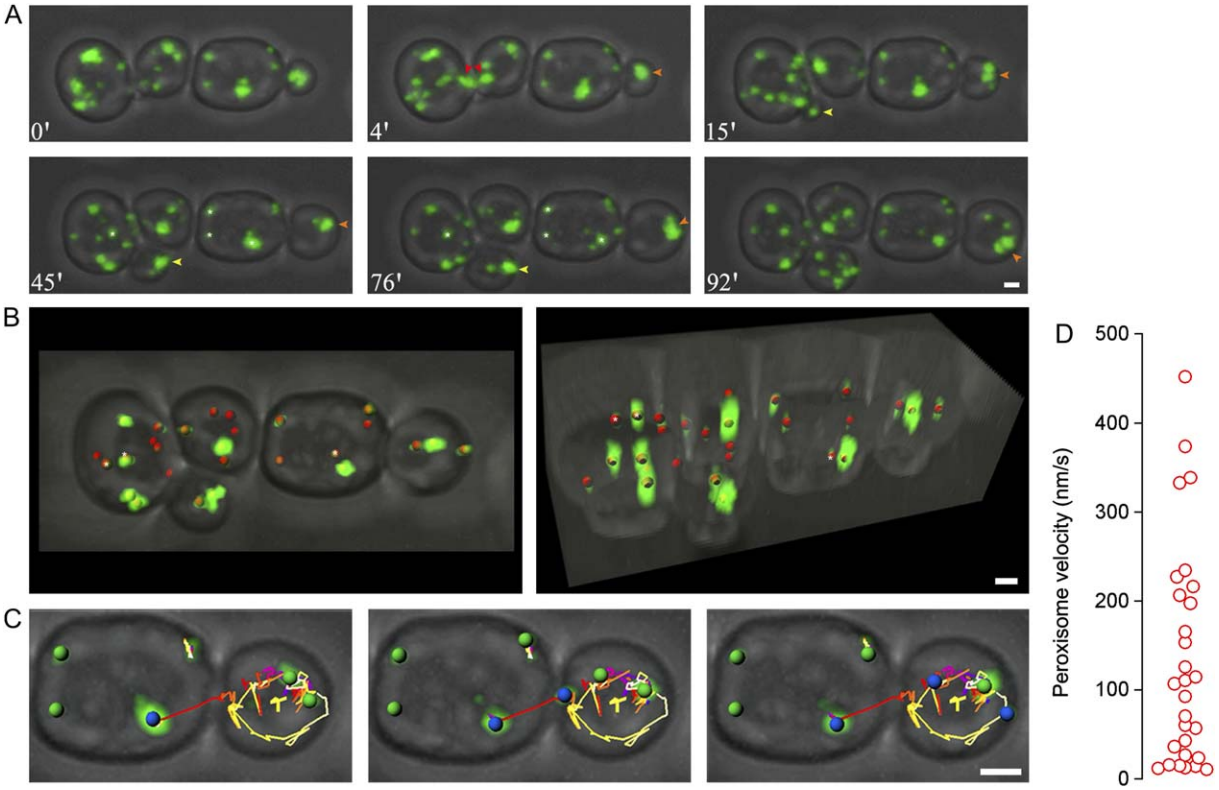

Figure 1. Peroxisome Dynamics in Wild-Type *S. cerevisiae* Cells

(A) Arrowheads point to peroxisomes labeled with Pot1p-GFP that clustered at sites of polarized growth. At 4 min, the cell at left underwent cytokinesis, and subsets of peroxisomes from both mother cell and bud relocated to the mother-bud neck region (red arrowheads). As soon as a new bud was visible (15′), peroxisomes within the mother cell lost their fixed positions and were inserted into the bud, where they clustered at the growing bud tip (yellow arrowhead). A cluster of peroxisomes localized to the bud tip is also visible in the bud at right (orange arrowhead). Asterisks mark some immobile peroxisomes in mother cells (Movie S1). Bar, 1 μm.

(B) Immobile peroxisomes are cortically localized. Three-dimensional reconstruction of a frame taken from Movie S1 (60'), when all peroxisomes in mother cells were immobile. Peroxisomes were marked by red spheres using Imaris 4.1. In three dimensions (right), all peroxisomes within mother cells clearly localize to the cell periphery. Asterisks mark cortical peroxisomes that appear in the middle of cells in 2-dimensional images (Movie S2). Bar, 1 μm.

(C) Peroxisome insertion into buds. Tracked peroxisomes were marked by blue spheres and other peroxisomes by green spheres using Imaris 4.1. A peroxisome detaches from the cortex and initially moves to the bud neck. Shortly after, it travels to the bud tip where it joins other inherited peroxisomes. The peroxisome shown here also divided following inheritance (Movie S3). Bar, 1 μm.

(D) Scatter plot of velocities of peroxisomes observed in Movie S1. Maximal velocity achieved by individual peroxisomes is presented.

organelles in wild-type and *inp2Δ* cells. The distribution of vacuoles was studied using the vacuole-specific fluorophore, FM4-64. The rates of vacuole inheritance in *inp2Δ* cells were essentially the same as those observed in wild-type cells (Figure 2B). The rates of inheritance of mitochondria, labeled by Sdh2p-GFP, were also unchanged in *inp2Δ* cells (Figure 2C). The orientation of mitotic spindles, labeled by GFP-Tub1p, was unimpaired in cells lacking Inp2p (Figure 2D).

We also analyzed the organization of the actin cytoskeleton in wild-type cells and cells lacking Inp2p. Actin was detected by staining with rhodamine-phalloidin. In wild-type and *inp2Δ* cells, actin showed normal polarized structures, with patches at sites of growth and distinct cables within mother cells (Figure 2E). Moreover, since *inp2Δ* cells displayed no growth defects on rich YPD medium (Figure 2F), Inp2p is not required for the polarized distribution of secretory vesicles. These findings collectively indicate that Inp2p is required specifically for peroxisome inheritance.

Inp2p Is a Peroxisomal Integral Membrane Protein Whose Levels Vary with the Cell Cycle

We used confocal fluorescence microscopy to determine the subcellular localization of a genomically encoded fluorescent chimera of Inp2p and GFP (Inp2p-GFP). Peroxisomes were visualized with a plasmid-encoded fluorescent chimera (mRFP-SKL) of monomeric red fluorescent protein (mRFP) and the peroxisome targeting signal 1, Ser-Lys-Leu. Inp2p-GFP colocalized with mRFP-SKL to punctate structures characteristic of peroxisomes (Figure 3A). Interestingly, the levels of Inp2p in individual peroxisomes varied dramatically, with peroxisomes in daughter cells having a much stronger Inp2p-GFP signal than peroxisomes in mother cells. Therefore, Inp2p seems to be preferentially enriched in peroxisomes that are delivered to the bud.

Subcellular fractionation also showed Inp2p to be peroxisomal. Similar to the peroxisomal matrix protein thiolase, a genomically encoded TAP chimera of Inp2p, Inp2p-TAP, localized preferentially to the organellar

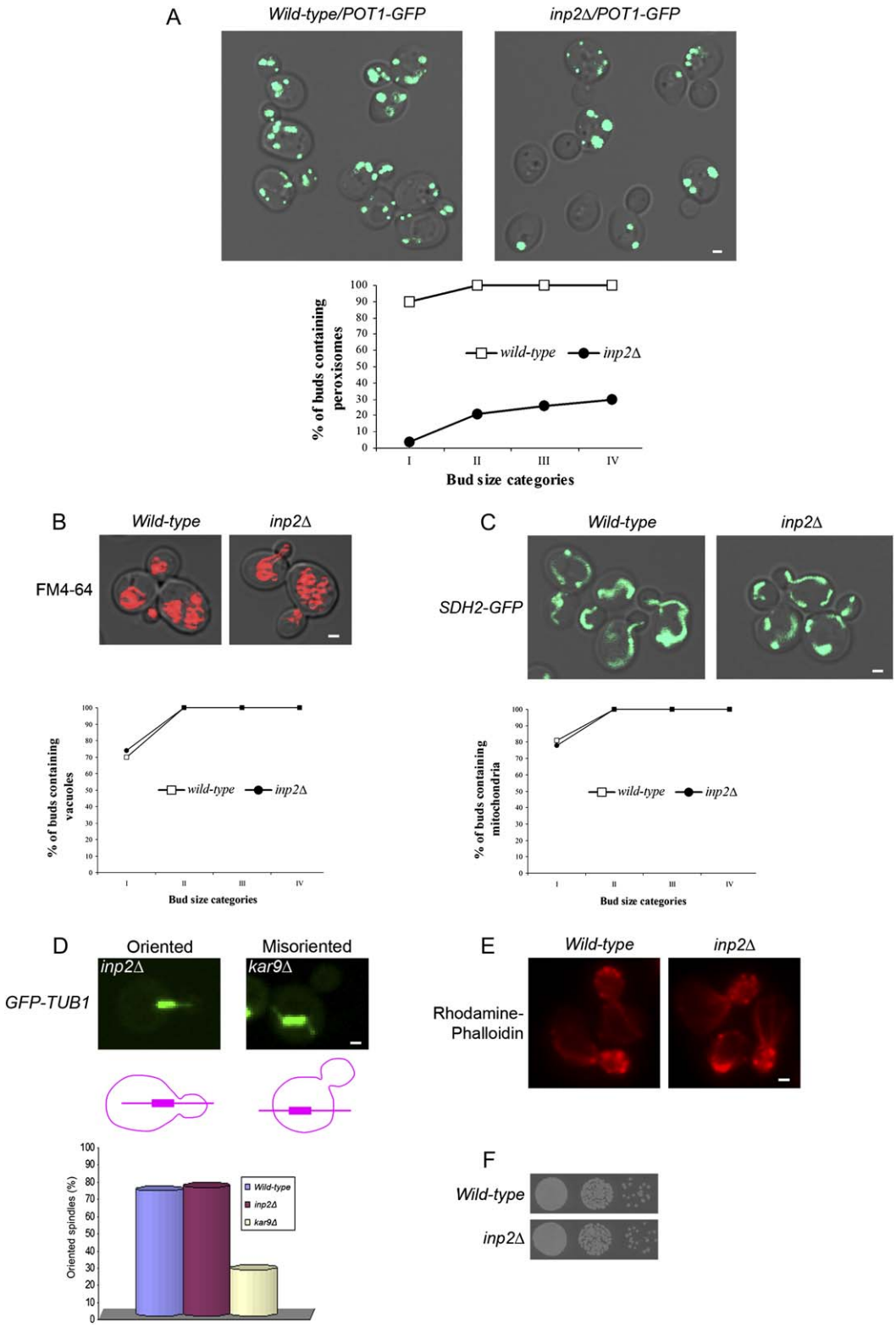

Figure 2. Deletion of the *INP2* Gene Affects Specifically Peroxisome Inheritance

(A) Wild-type and *inp2⊿* cells expressing *POT1-GFP* were incubated in SCIM for 16 hr. Fluorescent images of randomly chosen fields of cells were acquired as a stack by confocal microscopy. Buds were sized according to four categories relative to the volume of the mother cell (see Supplemental Experimental Procedures). The percentages of buds containing peroxisomes at each size category were plotted. Quantification was performed on at least 25 budded cells from each category. Bar, 1 μm.

(B) Vacuole inheritance is unaffected in *inp2⊿* cells. Vacuoles of wild-type and *inp2⊿* cells grown in YPD medium were labeled with the fluorophore FM4-64, and confocal images were captured. Quantification was performed as in (A). Bar, 1 μm.

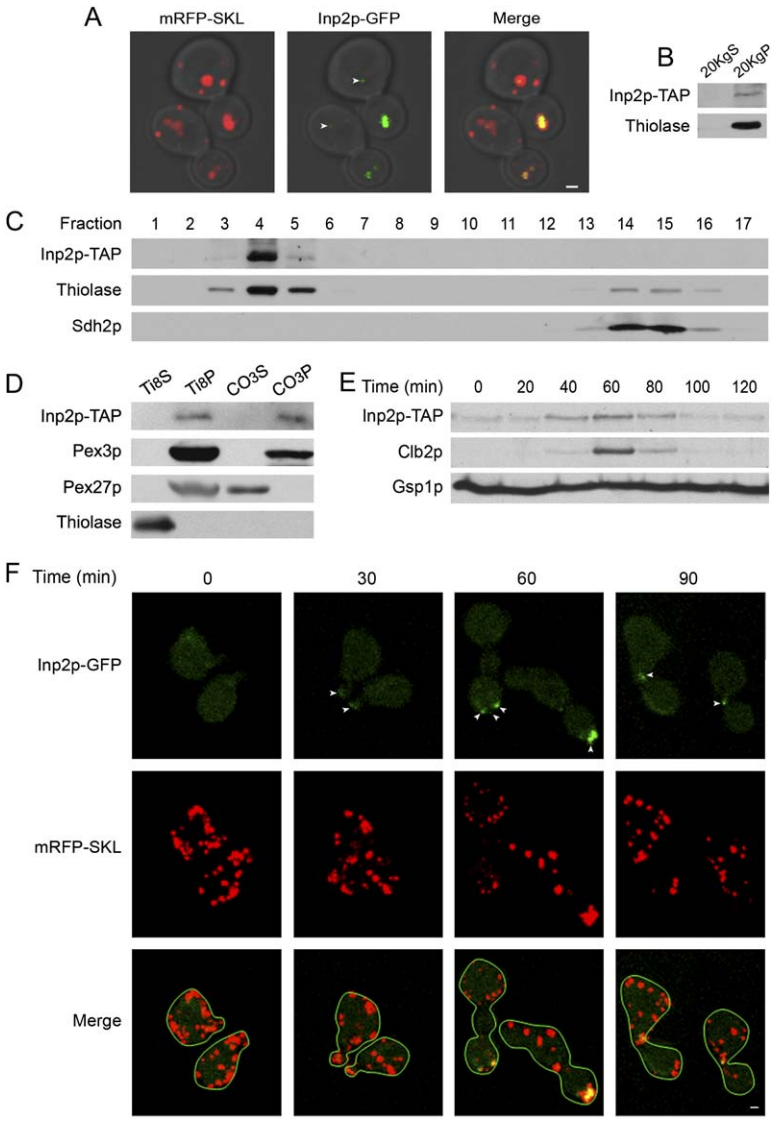

Figure 3. Inp2p Is a Peroxisomal Integral Membrane Protein Whose Levels Vary with the Cell Cycle

(A) Inp2p-GFP colocalizes with mRFP-SKL to punctate structures characteristic of peroxisomes by confocal microscopy. The panel at right presents the merged image of the left and middle panels. The weak Inp2p-GFP fluorescent signal in mother cells is indicated by arrowheads. Bar, 1 μm.

(B) Inp2p-TAP localizes to the peroxisome-enriched 20KgP subcellular fraction. Immunoblot analysis of equivalent portions of the 20KgS and 20KgP subcellular fractions from cells expressing Inp2p-TAP was performed with antibodies to the peroxisomal matrix enzyme, thiolase.

(C) Inp2p-TAP cofractionates with peroxisomes. Organelles in the 20KgP fraction were separated by isopycnic centrifugation on a discontinuous Nycodenz gradient. Fractions were collected from the bottom of the gradient, and equal portions of each fraction were analyzed by immunoblotting. Fractions enriched for peroxisomes and mitochondria were identified by immunodetection of thiolase and Sdh2p, respectively.

(D) Peroxisomes in a postnuclear supernatant fraction were ruptured by treatment with Ti8 buffer and subjected to ultracentrifugation to obtain a supernatant fraction (Ti8S) enriched for matrix proteins and a pellet fraction (Ti8P) enriched for membrane proteins. The Ti8P fraction was treated further with alkali Na_2CO_3 and separated by ultracentrifugation into a supernatant fraction (CO_3S) enriched for peripheral membrane proteins and a pellet fraction (CO_3P) enriched for integral membrane proteins. Equivalent portions of each fraction were analyzed by immunoblotting. Immunodetection of thiolase, Pex3p, and Pex27p marked the fractionation profiles of a peroxisomal matrix, integral membrane, and peripheral membrane protein, respectively.

(E) Cells expressing TAP-tagged Inp2p were grown for 16 hr in YPD medium and synchronized in G1 by addition of α factor. After removal of α factor, cells were incubated at 23ºC in YPD medium. Samples were collected at the times indicated, and total cell lysates were analyzed by immunoblotting with antibodies directed against the TAP tag, the cyclin Clb2p, or Gsp1p (Ran). Clb2p levels monitor the progression of synchronized cells through the cell cycle. Gsp1p serves as a control for protein loading.

(F) Cells synthesizing mRFP-SKL and Inp2p-GFP were treated as in (E). Fluorescent images of cells at different times after removal of α factor were captured with a spinning disk confocal microscope. The images represent projections of *z*-stacks of 14 optical sections spaced 0.4 μm apart. Arrowheads point to colocalization of Inp2p-GFP with peroxisomes at sites of growth. After removal of α factor (0 min), cells display mating projections (shmoos). At later time points, cells that formed buds at shmoo tips are shown. Bar, 1 μm.

pellet fraction (20KgP) enriched for peroxisomes and mitochondria (Figure 3B). Isopycnic density gradient centrifugation of the 20KgP fraction showed that Inp2p-TAP coenriched with thiolase but not with the mitochondrial protein Sdh2p (Figure 3C).

Organelle extraction showed Inp2p to be an integral membrane protein of peroxisomes. Similar to the peroxisomal integral membrane protein Pex3p and peripheral membrane protein Pex27p, Inp2p-TAP localized preferentially to the Ti8P fraction enriched for membrane

(C) Mitochondrial segregation is unaffected in *inp2Δ* cells. Wild-type and *inp2Δ* cells expressing *SDH2-GFP* were grown in YPD medium, and confocal images were captured. Quantification was performed as in (A). Bar, 1 μm.

(D) *inp2Δ* cells have properly oriented mitotic spindles. Wild-type, *inp2Δ* and *kar9Δ* cells genomically encoding a fluorescent chimera of α-tubulin, GFP-Tub1p, were grown as described (Adames et al., 2001) and visualized by confocal microscopy. The orientation of the mitotic spindle was analyzed in pre-anaphase cells as described (see Supplemental Experimental Procedures). Quantification was performed on at least 100 pre-anaphase budded cells of each strain. Bar, 1 μm.

(E) *inp2Δ* cells display a normal polarized actin cytoskeleton. Wild-type and *inp2Δ* cells were grown in YPD medium, and actin was detected with rhodamine-phalloidin and visualized by epifluorescence microscopy. Bar, 1 μm.

(F) Wild-type and *inp2Δ* cells show similar growth on glucose-containing medium. Strains were grown to mid-log phase in liquid YPD medium, and equal amounts of cells were serially diluted ten-fold onto YPD agar and incubated at 30ºC.

proteins (Figure 3D). Upon extraction of the Ti8P fraction with alkali Na_2CO_3, Inp2p-TAP cofractionated with Pex3p to the CO_3P fraction enriched for integral membrane proteins.

The levels of mRNA coding for Inp2p have been reported to fluctuate with the cell cycle (Spellman et al., 1998). The observed enrichment of Inp2p in peroxisomes found in the bud raised the possibility that the levels of Inp2p itself might fluctuate with the cell cycle. To test this, we analyzed the levels of Inp2p-TAP in cells subjected to and released from α factor-induced G1 arrest. Inp2p-TAP levels did vary with the cell cycle, increasing 40 min after and decreasing 80 min after α factor release (Figure 3E).

We investigated the dynamics of Inp2p during the cell cycle further by analyzing the levels and localization of Inp2p-GFP in cells released from α factor-induced G1 arrest (Figure 3F). The Inp2p-GFP signal is below the threshold of detection immediately after removal of α factor (Figure 3F, 0 min), and only cytoplasmic autofluorescence is seen. In small budded cells (Figure 3F, 30 min), Inp2p-GFP fluorescence becomes detectable and colocalizes with peroxisomes delivered to the buds, which, at this stage, are concentrated at bud tips. Inp2p-GFP fluorescence is significantly increased in large budded cells and is present on those peroxisomes that congregate at bud tips (Figure 3F, 60 min). Some peroxisomes in mother cells also contain detectable levels of Inp2p-GFP. The Inp2p-GFP signal is weak at cytokinesis and concentrated in those peroxisomes from the bud and mother cell that relocate to the mother-bud neck region (Figure 3F, 90 min).

Inp2p Interacts Directly with the Globular Tail of Myo2p

We performed yeast two-hybrid analysis to test the ability of Inp2p to interact with the carboxy-terminal globular domain of Myo2p (amino acids 1113-1574). A strong interaction was detected between Inp2p and the Myo2p globular domain (Figure 4A). We also confirmed a known interaction between Inp2p and Pex19p (Ito et al., 2001). Pex19p has been shown to be involved in the targeting/stabilization of proteins to/in the peroxisomal membrane (Schliebs and Kunau, 2004). No interaction was detected between Inp2p and Inp1p.

To define regions of Inp2p involved in binding the Myo2p tail, we generated Inp2p deletion mutants and tested them in the two-hybrid system (Figure 4B). The region between the two coiled-coil domains of Inp2p (amino acids 504-618) interacted weakly with the Myo2p tail. In contrast, the entire portion of Inp2p carboxy-terminal to the predicted transmembrane domain (amino acids 240-705) bound Myo2p as strongly as full-length Inp2p, suggesting that other regions within this fragment are important for the interaction between Inp2p and the Myo2p tail.

If Inp2p is the bona fide peroxisomal receptor for Myo2p, we expect it to interact directly with Myo2p. Since yeast two-hybrid analysis does not differentiate between direct and bridged protein interactions, we performed a GST pull-down assay using recombinant Inp2p and Myo2p tail made in *Escherichia coli* (Figure 4C). To improve the solubility of the maltose binding protein (MBP) fusion with Inp2p (MBP-Inp2p), only amino acids 241–705 of Inp2p were fused to MBP, thereby excluding the hydrophobic region of Inp2p (amino acids 211-239) but still preserving the region between amino acids 240 and 705 capable of interacting with Myo2p (Figre 4B). MBP-Inp2p was pulled down by GST-Myo2p but not GST alone (Figure 4C). Also, MBP alone or MBP fused to either Inp1p or Vam2p, proteins whose functions are unrelated to Myo2p, did not show an interaction with GST-Myo2p or GST alone. These results show that Inp2p binds directly that part of Myo2p specialized in cargo association.

Peroxisome Inheritance Is Abolished or Delayed in Cells Lacking Inp2p

4D video microscopy showed that peroxisome inheritance in cells lacking Inp2p was either abolished or significantly delayed (Figure 5; Movies S4–S7). During bud growth, peroxisomes appeared immobile at cortical locations within the mother cell and generally failed to be transferred to the bud (Figure 5A; Movie S4). In other cases, a subset of peroxisomes within the mother cell exhibited random movement but still failed to be efficiently localized to the bud (Figures 5B and 5C; Movies S5 and S6). Overall, peroxisomes in cells lacking Inp2p moved more slowly and in a less directed manner compared to peroxisomes in wild-type cells (Figure S1). Consistent with our quantification of peroxisome inheritance (see Figure 2), we also observed peroxisomes being transferred to buds. Interestingly, in most cases, only one peroxisome would be delivered to the bud, and this event would take place with significant delay after emergence of the bud (Figures 5C and 5D; Movies S6 and S7). Notably, upon cytokinesis, we never observed relocation of peroxisomes from mother cells or buds to the mother-bud neck region (Figures 5A–5C; Movies S4–S6). Moreover, after peroxisomes reached the buds of *inp2Δ* cells, they did not show a preference for sites of polarized growth (Figures 5B–5D; Movies S5–S7). Quantification showed that only 23% of *inp2Δ* buds containing peroxisomes displayed peroxisomal fluorescence at bud tips compared to 78% of buds of wild-type cells (Figure 5E).

Peroxisome Movements within Buds of *inp2Δ* Cells Are Not Dependent on the Acto-Myosin System

The inability of peroxisomes to localize to bud tips in *inp2Δ* cells might result from their failure to associate with the acto-myosin system. Many yeast organelles are translocated to the bud by Myo2p along actin cables that extend to the bud tip (Rossanese et al., 2001; Ishikawa et al., 2003). Moreover, the congregation of organelles at the bud tip is also dependent on Myo2p (Rossanese et al., 2001; Boldogh et al., 2004), which presumably tethers them to actin structures localized at the bud tip.

We investigated whether the acto-myosin system plays a similar role in peroxisome movement within buds. We first analyzed the movements of peroxisomes in *bni1Δ* cells, which have significantly less actin cables inside buds (Pruyne et al., 2004). 4D video microscopy showed that peroxisomes in *bni1Δ* cells were recruited from the mother cell but tended to accumulate at the mother-bud neck (Figure 5F; Movie S8). On occasion, peroxisomes associated with the bud cortex but never

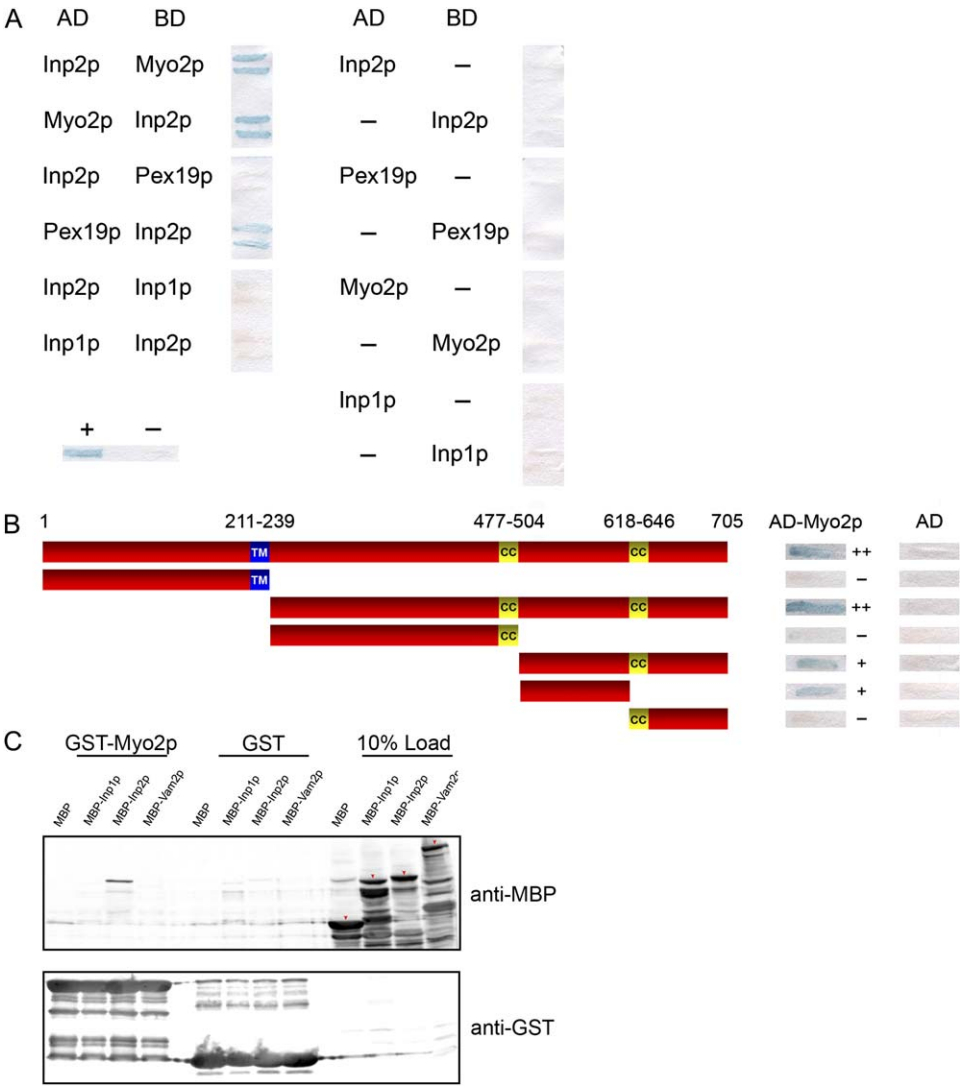

Figure 4. Inp2p Interacts Directly with the Globular Tail of Myo2p

(A) *S. cerevisiae SFY526* cells synthesizing both Gal4-AD and Gal4-BD protein fusions to Inp2p, the tail of Myo2p (amino acids 1113-1574), Pex19p, and Inp1p were tested for their ability to interact with each other by a β-galactosidase filter detection assay. A positive interaction is detected by the production of blue color. The color intensities of controls for the presence (+) or absence (−) of a protein interaction are presented at bottom, left. No construct is auto-activating, since no β-galactosidase activity is detected for cells synthesizing only one fusion protein (right).

(B) Two hybrid analysis was performed as in (A) to test the ability of the indicated regions of Inp2p to interact with the globular tail of Myo2p. TM = predicted transmembrane region. CC = predicted coiled-coil region. No construct is auto-activating (AD). A strong interaction is denoted by two plus signs (++), while a weak interaction is denoted by one plus sign (+). The absence of an interaction is denoted by a minus sign (−).

(C) Glutathione sepharose beads containing either GST fused to the cargo binding tail of Myo2p (GST-Myo2p) or GST alone were incubated with extracts of *E. coli* synthesizing MBP, MBP-Inp1p, MBP-Inp2p, or MBP-Vam2p. Bound proteins, as well as 10% of input proteins, were analyzed by immunoblotting with anti-MBP antibodies (upper panel). Arrowheads highlight full-length MBP or MBP fusion proteins. Total GST-Myo2p or GST protein levels were visualized by immunoblotting with anti-GST antibodies (lower panel).

clustered at bud tips. In fact, bud tips were frequently devoid of peroxisomes. Only 20% of *bni1Δ* cells displayed peroxisomes at bud tips as compared to 78% of wild-type cells (Figure 5H). Actin cables are therefore required for targeting peroxisomes to bud tips.

myo2-66 cells carry a conditional mutation in the Myo2p motor domain. These cells exhibit severe defects in the inheritance of vacuoles (Hill et al., 1996), late Golgi (Rossanese et al., 2001), and peroxisomes (unpublished data) even at room temperature. Video microscopy of *myo2-66* cells at 24ºC (Figure 5G; Movie S9) showed a significant delay in the insertion of peroxisomes into buds, consistent with the role for Myo2p in the movement of peroxisomes (Hoepfner et al., 2001). After peroxisomes reached the bud tips, they usually did not remain there and sometimes returned to mother cells. Quantification showed that only 38% of *myo2-66* buds containing peroxisomes displayed peroxisomes at bud tips (Figure 5H). Irrespective of mechanism, these data collectively suggest that the acto-myosin system functions in both targeting peroxisomes to sites of growth and maintaining them at these sites. Therefore, the

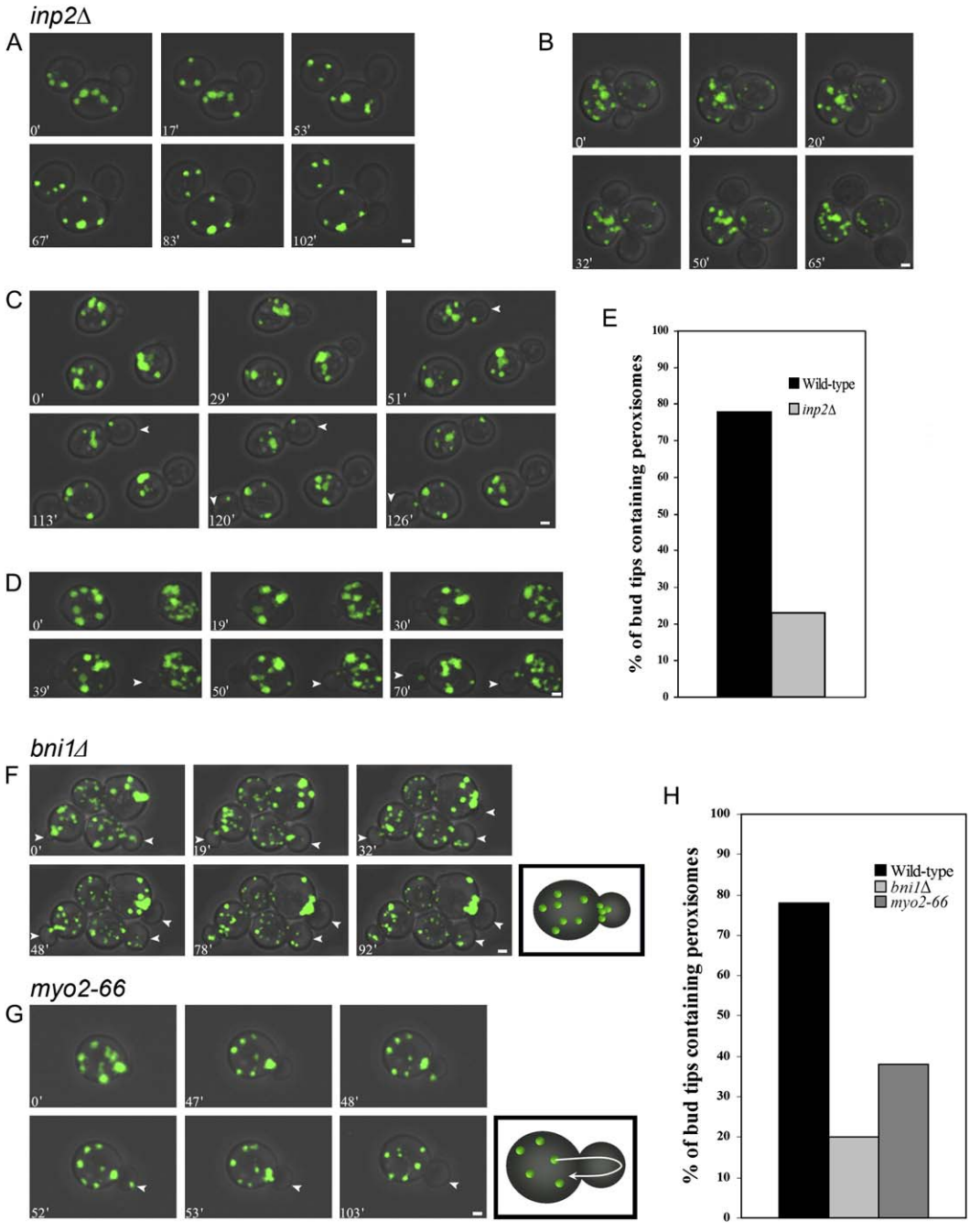

Figure 5. Peroxisome Dynamics in *inp2Δ*, *bni1Δ*, and *myo2-66* Cells

(A and B) Abolished peroxisome inheritance in *inp2Δ* cells.

(A) In this movie, the bud does not receive peroxisomes before cytokinesis. The next bud shares the same fate as the first and does not receive peroxisomes (67' -102'). All peroxisomes in the mother cell retain fixed positions. (Movie S4).

(B) At the beginning of this movie (0'), the bud at top is devoid of peroxisomes, while there is a single peroxisome in the bud at bottom. This peroxisome will return to the mother cell (9'). During bud growth, no peroxisome is inserted into either bud. Some peroxisomes in the mother cells perform chaotic movements (Movie S5).

(C and D) Delayed peroxisome inheritance in *inp2Δ* cells. A few peroxisomes are delivered to the buds with significant delay. These peroxisomes do not show a preference for bud tips (Movies S6 and S7). Arrowheads point to bud tips devoid of peroxisomes.

(E) Quantification of peroxisomes at bud tips. Wild-type and *inp2Δ* cells expressing *POT1-GFP* were incubated for 16 hr in SCIM. Only buds containing peroxisomes were analyzed. The percentages of buds containing peroxisomes at the bud tips were calculated.

(F–H) Peroxisome movements within buds are dependent on the acto-myosin system.

(F) Peroxisome dynamics in *bni1Δ* cells. Peroxisomes tend to accumulate at the bud neck, as seen in the cell and its associated bud at top, right (32'-92'). Peroxisomes can also sometimes enter the bud and associate along the bud cortex, as seen in the cell and its associated bud at bottom, right (19'-92'). Arrowheads indicate bud tips devoid of peroxisomes (Movie S8).

observed chaotic movements of peroxisomes within the buds of cells lacking Inp2p most likely reflect their lack of attachment to the acto-myosin system, which is unaltered in this mutant.

Overexpression of *INP2* Leads to the Depletion of Peroxisomes from Mother Cells

We showed that peroxisomes in buds have more Inp2p than peroxisomes in mother cells (Figure 3A). This asymmetric distribution of Inp2p could reflect a relationship between the quantity of Inp2p on an individual peroxisome and its ability to be transferred to the bud by Myo2p. Such a scenario leads to the prediction that overproducing Inp2p should enable an increased number of peroxisomes to be transported to the bud. We determined whether this was the case by overexpressing *INP2* from the multicopy plasmid YEp13 in wild-type cells synthesizing Pot1p-GFP.

As predicted, budded cells of the strain overproducing Inp2p had most of their peroxisomes localized to the buds (Figure 6A). Moreover, a significant percentage of mother cells were devoid of peroxisomes. This asymmetric distribution of peroxisomes, with the entire peroxisomal population present in the bud, was never observed in wild-type cells containing the parental plasmid YEp13 alone (Figure 6A). Quantification showed that cells overproducing Inp2p exhibited an increased percentage of mother cells without peroxisomes with increasing bud size, with 9% of mother cells with the smallest buds (Category I) and 32% of mother cells with the largest bud (Category IV) lacking peroxisomes (Figure 6A).

4D video microscopy showed that in a cell overproducing Inp2p, the entire population of peroxisomes was found concentrated at the site of polarized growth. As soon as the bud was visible, most of the peroxisomes accumulated at the site of bud emergence and were then inserted into the bud (Figure 6B; Movie S10). The few cortically anchored peroxisomes in the mother cell were also recruited and transferred to the bud, thereby depleting the mother cell of peroxisomes. Once in the bud, all peroxisomes clustered at the bud tip. In contrast to wild-type cells, all peroxisomes relocated en masse from the bud tip to the bud-neck region upon cytokinesis.

Colocalization studies between peroxisomes and Myo2p showed that in wild-type cells, only a small number of peroxisomes colocalized with Myo2p at sites of polarized growth, while the majority of peroxisomes were found within the mother cell (Figure 6C, upper panels). In contrast, in cells overproducing Inp2p, the entire population of peroxisomes associated with Myo2p at sites of polarized growth, sometimes as soon as bud formation was apparent (Figure 6C, lower panels).

The segregation of vacuoles and mitochondria was unaffected in cells overproducing Inp2p (Figures 6D and 6E). Mitotic spindles were also oriented properly in cells overproducing Inp2p (Figure 6F).

The Interplay between Inp2p and Inp1p

The transfer of all peroxisomes from mother cell to bud has also been observed in cells lacking Inp1p, a protein that anchors peroxisomes to the mother cell cortex (Fagarasanu et al., 2005). Overproducing Inp2p in cells lacking Inp1p led to the more rapid appearance of peroxisomes in buds than in *inp1Δ* cells or wild-type cells overproducing Inp2p (Figure 7A). The opposite was observed in *inp2Δ* cells overexpressing *INP1*, as the percentage of buds lacking peroxisomes was greater at all bud size categories in these cells than in either *inp2Δ* cells or wild-type cells overexpressing *INP1* (Figure 7B). Therefore, the effect of overproducing either of these two apparently counteracting proteins is enhanced by the absence of the other protein.

To gain further insight into the interplay between Inp1p and Inp2p, we constructed cells deleted for both *INP1* and *INP2*. We observed a large number of buds of *inp1Δ/inp2Δ* cells that lacked peroxisomes. However, the percentages of budded cells lacking peroxisomes within buds were lower than those observed for cells lacking Inp2p alone but still greater than those observed for wild-type cells (Figure 7C). Notably, no *inp1Δ/inp2Δ* budded cell was observed that had its entire complement of peroxisomes within its bud, a feature characteristic of *inp1Δ* cells.

Discussion

Given the many different types of membrane-bound organelles in a eukaryotic cell, ensuring their correct delivery to a specific destination at a specific time requires a tightly regulated transport system. The intracellular transport of organelles is supported by either microtubule or actin networks and powered by motor proteins that associate with these networks. How motor proteins recognize their target organelles and what the molecular basis is for the temporal and spatial regulation of this recognition are important questions in cell biology.

Class V myosins are the most effective and processive members of the myosin superfamily that participate in actin-mediated organelle motility (Rief et al., 2000). These unconventional myosins have medical importance. Mutations in the myosin Va gene cause Griscelli syndrome type I (Pastural et al., 1997), an ultimately lethal condition characterized by hypopigmentation and central nervous system dysfunction. Class V myosins attach to their cargoes by interacting with adaptor "receptor" molecules on the surface of a target organelle. Only two such receptors, both residing on organelles of the lysosome family, have been characterized: melanophilin on melanosomes (Wu et al., 2002) and Vac17p on the yeast vacuole (Ishikawa et al., 2003).

In *S. cerevisiae*, the movement of each organelle during the cell cycle has specific temporal and spatial characteristics, despite the fact that most of these organelles are carried by the same motor protein, the class V myosin Myo2p. This promiscuity in organelle movement by Myo2p has been explained by the existence of

(G) Peroxisome dynamics in *myo2-66* cells. Peroxisomes remain anchored at the cortex of the mother cell. After significant delay (48'), one peroxisome is transported to the bud. This peroxisome is initially correctly localized to the bud tip (arrowhead) but subsequently leaves the bud (53') (Movie S9).

(H) Quantification of the presence of peroxisomes at bud tips was performed as described in the legend to panel (E).

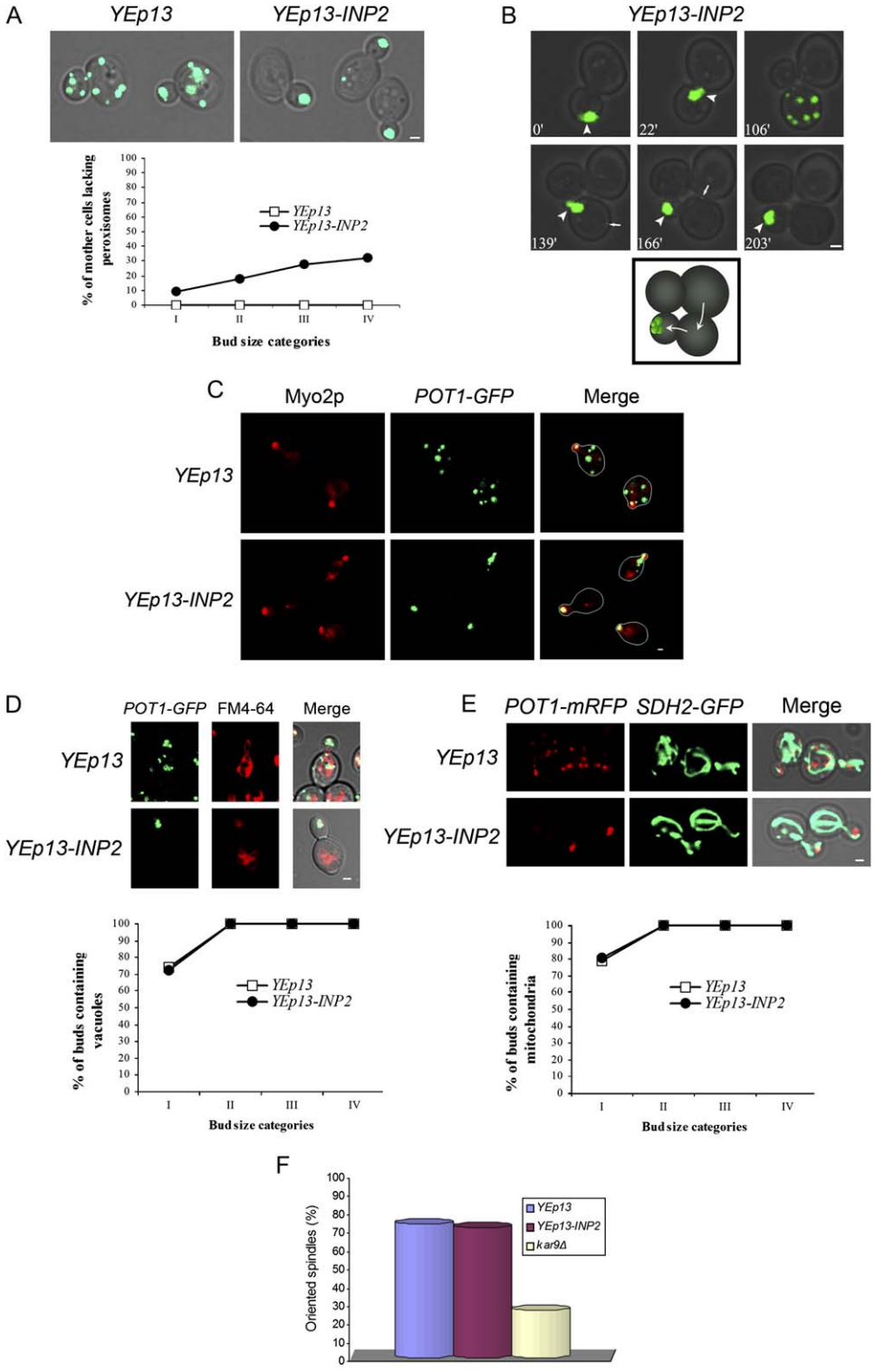

Figure 6. Overproduction of Inp2p Alters the Partitioning of Peroxisomes without Affecting the Segregation of Other Organelles

(A) Wild-type and *INP2*-overexpressing cells synthesizing Pot1p-GFP were incubated in SCIM and examined by confocal microscopy as described in the legend to Figure 2. Scoring for the presence or absence of peroxisomes in buds of different sizes and in mother cells was performed on at least 25 budded cells from each category of bud size. Bar, 1 μm.

(B) Peroxisome dynamics in cells overproducing Inp2p. Arrowheads point to peroxisomes clustered at sites of polarized growth. Imaging was initiated after all peroxisomes had been delivered to the bud. The peroxisomes in the bud form a cluster at the bud tip (0'). At cytokinesis (22′), all peroxisomes move *en masse* to the mother-bud neck region (arrowhead). Later in the cell cycle, peroxisomes detach from one another and are found scattered in the former bud (106'). As soon as the cell containing peroxisomes forms a new bud (139'), peroxisomes relocate to the presumptive bud site (arrowhead) and are then inserted into the bud (166'), where they localize to the bud tip (arrowhead). One small peroxisome (arrow) remains anchored at the mother cell cortex for about 20 min. This peroxisome will be recruited from its fixed position (166') and move into the bud (Movie S10).

organelle-specific receptors for Myo2p that are regulated according to cell cycle cues. Vac17p was the first such receptor identified, functioning as the vacuole-specific receptor for Myo2p (Ishikawa et al., 2003). Following this reasoning, we set out to identify the Myo2p receptor on peroxisomes. We found that Inp2p possesses the attributes of a peroxisome-specific receptor for Myo2p.

Inp2p is a peroxisomal membrane protein that interacts directly with the cargo binding globular tail of Myo2p and is essential for the segregation of peroxisomes to growing buds. The segregation of other organelles is unaffected by deletion of the *INP2* gene, eliminating the possibility of a role for Inp2p in cell polarity or in organization of the actin cytoskeleton. The levels of Inp2p oscillate with the cell cycle in a pattern that corresponds to the dynamics of peroxisomes. Moreover, the localization of Inp2p changes with the cell cycle, preferentially marking those peroxisomes that are distributed to sites of growth by Myo2p. In addition, upon overproduction of Inp2p, the entire peroxisome population becomes concentrated at those intracellular sites at which Myo2p normally accumulates. All these findings strongly suggest Inp2p as the link between peroxisomes and Myo2p. The discovery of Inp2p as the peroxisome-specific receptor for Myo2p supports the proposition that different organelles have different specific Myo2p receptors.

Inp2p was enriched preferentially in peroxisomes that were transferred to the bud. Since Inp2p is essential for the directed movement of peroxisomes, its asymmetric distribution could indicate that Myo2p selectively transports those peroxisomes with increased amounts of Inp2p, effectively establishing an Inp2p gradient along the mother-bud axis. We propose that the attainment of a certain level of Inp2 on a given peroxisome enables the Inp2p-Myo2p transport complex to displace that peroxisome from its attachment site at the mother cell cortex and move it rapidly to the bud (Figure 7D).

Inp2p exhibits the characteristics of an integral membrane protein of peroxisomes and is predicted to contain one membrane-spanning region at amino acids 211-239. This distinguishes Inp2p from the two myosin V receptors, melanophilin and Vac17p, which are peripheral membrane proteins that require an additional membrane protein to mediate their attachment to the organelle membrane (Wu et al., 2002; Tang et al., 2003). However, Inp2p and Vac17p share common features that could be used as criteria to screen for class V myosin receptors on other yeast organelles, including cortical ER (Estrada et al., 2003), late Golgi elements (Rossanese et al., 2001) and secretory vesicles (Schott et al., 1999). Both Inp2p and Vac17p have two coiled-coil domains that are each about 30 amino acid residues in length. Tandem coiled-coil domains of about the same size are also found in melanophilin (Nagashima et al., 2002) and may represent a common feature of all organelle receptors for class V myosins. The levels of Inp2p and Vac17p, and those of their corresponding mRNAs, oscillate during the cell cycle in a pattern that parallels the dynamics of yeast organelles (Tang et al., 2003), strongly suggesting that the amount of class V myosin receptor associated with an organelle at each point of the cell cycle is crucial to the regulation of the movement of that organelle.

We observed that a number of buds in the *inp2Δ* strain contained peroxisomes. One possibility for this observation is that even in the absence of Inp2p, peroxisomes retain some affinity for Myo2p, which, on occasion, enables a few peroxisomes to be inserted into the bud. However, these peroxisomes do not exhibit the Myo2p-dependent movements exhibited by peroxisomes in buds of the wild-type strain. A second possibility is that peroxisomes are carried into the buds of *inp2Δ* cells by the efflux of other organelles.

We also analyzed peroxisome dynamics in *inp2Δ* mother cells. While the majority of peroxisomes were static, some peroxisomes did move. However, much of this movement was chaotic, as opposed to the fast, directed, vectorial movements of peroxisomes observed in wild-type cells. The velocities of wild-type peroxisomes in their Myo2p-driven transit in mother cells varied widely, with a maximal observed velocity of 0.45 μm/s. Interestingly, Myo2p moves vacuoles at a velocity of 0.1–0.2 μm/s (Weisman, 2003), secretory vesicles at 3 μm/s (Schott et al., 2002), and microtubule ends at 1.22 μm/s (Hwang et al., 2003). These differences in the velocities with which Myo2p carries various cargoes most probably reflect the different drags associated with the transport of cargoes of different shapes and sizes (Weisman, 2003). While no homolog of Inp2p apparently exists in higher eukaryotes, understanding the Myo2p-Inp2p interaction and how it is regulated will enable the development of testable predictions regarding motor-cargo interactions in general.

What is the relationship of Inp2p to Inp1p, the previously characterized peroxisomal protein involved in peroxisome inheritance? Inp1p and Inp2p are two key regulators of peroxisome inheritance with apparently antagonistic functions. In wild-type cells, about half of the peroxisomes is retained within the mother cell, a process dependent on Inp1p (Fagarasanu et al., 2005), while the other half is transported to the bud in an

(C) Overproduction of Inp2p leads to enhanced recruitment of peroxisomes to sites of polarized growth. Wild-type cells overexpressing *INP2* (*YEp13-INP2*) or containing the parental plasmid (*YEp13*) and synthesizing Pot1p-GFP were incubated in SCIM. Cells were processed for immunofluorescence microscopy with antibody to Myo2p. Primary anti-Myo2p antibody was detected with rhodamine-conjugated secondary antibody. Panels at right show the merge of signals from GFP and rhodamine. Bar, 1 μm.

(D) Vacuole segregation is unaffected by overproduction of Inp2p. Wild-type and *INP2*-overexpressing cells synthesizing Pot1p-GFP were incubated in SCIM. Vacuoles were labeled with FM4-64, and cells were analyzed by confocal microscopy. The panels at right show the merge of signals from GFP and FM4-64. Quantification was performed on at least 25 budded cells from each category of bud size. Bar, 1 μm.

(E) Mitochondria segregation is unaffected by overproduction of Inp2p. Wild-type and *INP2*-overexpressing cells synthesizing Pot1p-mRFP and Sdh2p-GFP were incubated in SCIM and analyzed by confocal microscopy. The panels at right show the merge of signals from mRFP and GFP. Quantification was performed on at least 25 budded cells from each category of bud size. Bar, 1 μm.

(F) Orientation of the mitotic spindle is unaffected by overproduction of Inp2p. Pre-anaphase wild-type, *INP2* overexpressing, and *kar9Δ* cells synthesizing GFP-Tub1p were analyzed for orientation of the mitotic spindle as described in the legend to Figure 2D. Quantification was performed on at least 100 pre-anaphase budded cells of each strain. Bar, 1 μm.

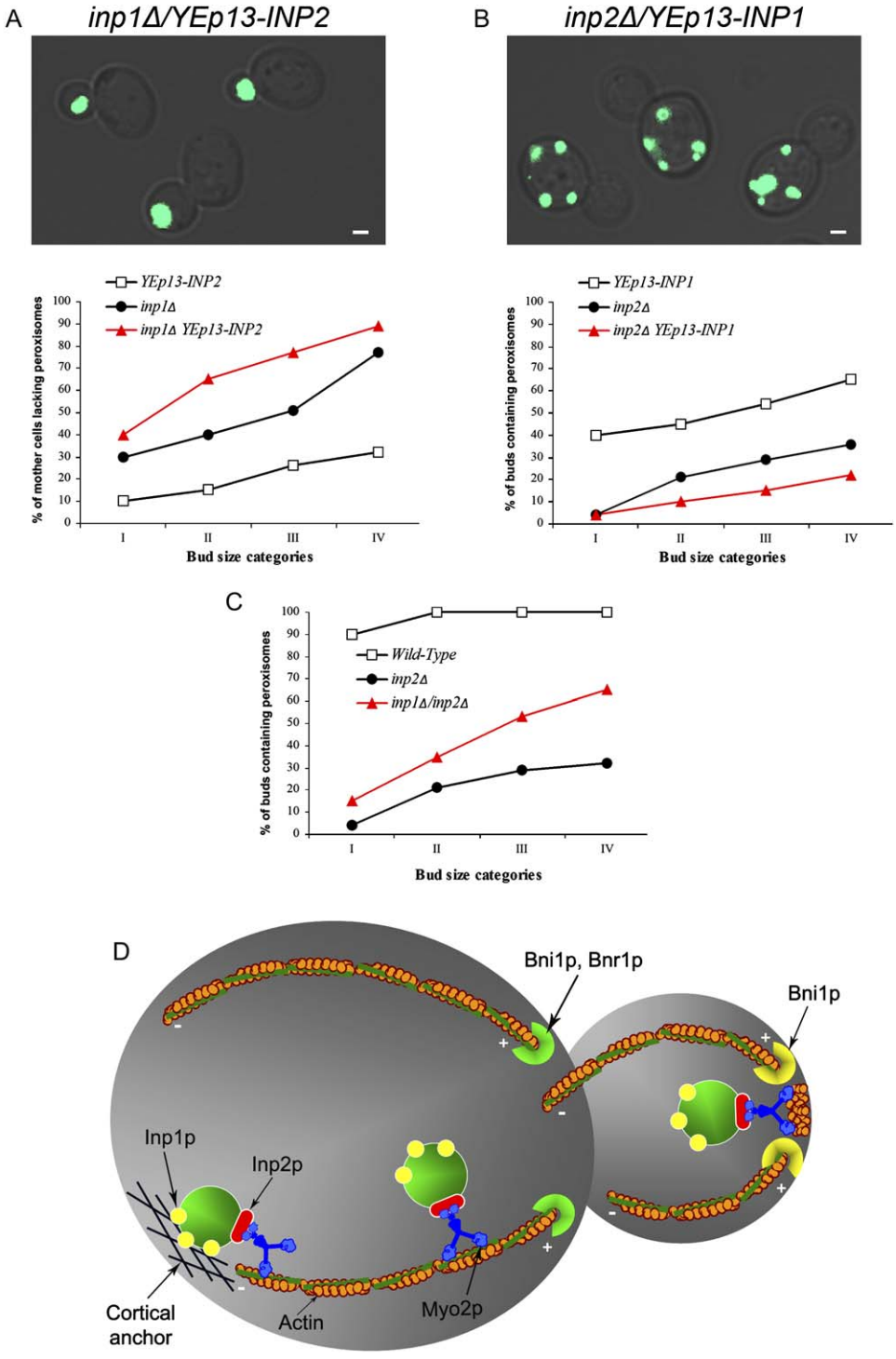

Figure 7. Interplay between Inp1p and Inp2p

(A–C) The indicated strains were incubated and subjected to quantification of peroxisome inheritance as described in the legend to Figure 2A. Bar, 1 μm.

(D) A model for Inp2p function in peroxisome inheritance. At a point in the cell cycle, Inp2p is synthesized and loaded onto peroxisomes. The increased levels of Inp2p on some peroxisomes result in the formation of Inp2p-Myo2p transport complexes that can dislodge these peroxisomes from their fixed cortical positions. The Inp2p-Myo2p complexes move the attached peroxisomes along polarized actin cables. Once in the bud, the Inp2p-Myo2p complexes are long-lived and responsible for localizing peroxisomes to sites of active growth, where Myo2p is concentrated. The regulated turnover of Inp2p later in the cell cycle results in detachment of peroxisomes from the Myo2p motor. As a result, only a subset of peroxisomes follows Myo2p to the mother-bud neck at cytokinesis. To prepare the bud for the ensuing cell cycle, peroxisomes become anchored at the bud cortex, a process dependent on Inp1p (not depicted).

Inp2p-dependent manner. Some insight into the interplay between Inp1p and Inp2p can be gained by studying the behavior of peroxisomes in cells overproducing or lacking one of these two key regulators of peroxisome inheritance. In cells overproducing Inp1p, all peroxisomes assume static cortical positions within the mother cell, even though the cells contain Inp2p (Fagarasanu et al., 2005). In contrast, overproduction of Inp2p in the presence of Inp1p leads to the Myo2p-dependent targeting of all peroxisomes to the bud and depletion of the peroxisome population in the mother cell. Thus, the overproduction of one of these proteins negates the function of the other. Moreover, the effects caused by overexpression of either *INP1* or *INP2* are enhanced by the lack of the other gene.

These scenarios suggest that there is a tug-of-war for peroxisomes between Inp1p, which acts to anchor peroxisomes in cells, and Inp2p-Myo2p, which moves peroxisomes, to determine the fate of individual peroxisomes during the cell cycle. Regulatory mechanisms therefore ultimately act to balance these molecular "contests of strength" to ensure that approximately half of the peroxisome population dissociates from the mother cell cortex to be transported to the bud (Figure 7D).

Interestingly, in *inp1Δ* cells, no peroxisomes had fixed positions at the mother cell cortex, which often resulted in the complete transfer of the peroxisome population to the daughter cell (Fagarasanu et al., 2005). It can be assumed that each peroxisome in *inp1Δ* cells has sufficient Inp2p to recruit Myo2p and promote its directed movement to the bud in the absence of an opposing force. In *inp1Δ/inp2Δ* cells, peroxisomes are left without any means of anchoring to the cell cortex and any possibility of attaching to the translocation machinery, which probably leads to a random distribution of peroxisomes. The presence, under these conditions, of buds devoid of peroxisomes probably reflects the inefficiency of stochastic segregation of peroxisomes in a cell that divides by budding.

In closing, we have shown that the peroxisomal membrane protein Inp2p is directly involved in the Myo2p-driven transport of peroxisomes to the bud during cell division in *S. cerevisiae* and exhibits the hallmarks of a peroxisome-specific receptor for the class V myosin, Myo2p.

Experimental Procedures

Strains and Culture Conditions

S. cerevisiae strains used in this study are listed in Table S1. Strains were cultured at 30ºC, unless otherwise indicated. Strains containing plasmids were cultured either in synthetic minimal (SM) medium or, if induction of peroxisomes was needed, in SCIM without leucine. Media components were YPD, 1% yeast extract, 2% peptone, 2% glucose; SCIM, 0.67% yeast nitrogen base without amino acids, 0.5% yeast extract, 0.5% peptone, 3.3% Brij 35, 0.1% glucose, 0.1% oleic acid, 1×complete supplement mixture (Bio 101) with or without leucine; YPBO, 0.3% yeast extract, 0.5% peptone, 0.5% K_2HPO_4, 0.5% KH_2PO_4, 3.3% Brij 35, 1% oleic acid; SM, 0.67% yeast nitrogen base without amino acids, 2% glucose, 1× complete supplement mixture without uracil or leucine.

Microscopy

Unless otherwise indicated, strains viewed by fluorescence microscopy were grown to mid-log phase in YPD or SM medium and then incubated in SCIM for 16 hr. Images were captured with a Plan-Apochromat 63×/1.4 NA oil DIC objective and an Axiovert 200 microscope equipped with either a LSM 510 META confocal scanner (Carl Zeiss) or, in the case of GFP-Tub1p and Inp2p-GFP, an Ultraview ERS spinning disc confocal imager (Perkin Elmer) and an ORCA-ER camera (Hamamatsu). Actin structures were visualized using a Model BX50 epifluorescence microscope (Olympus) equipped with a digital fluorescence camera (Spot Diagnostic Instruments).

Supplemental Data

Supplemental data including a supplemental figure, a supplemental table, additional Experimental Procedures, and ten supplemental movies are available at http://www.developmentalcell.com/cgi/content/full/10/5/587/DC1/.

Acknowledgments

We thank Drs. Benjamin Glick, Adam Hammond, Neil Adames, and Xuejun Sun for help with 4D video microscopy and Dr. Andrew Simmonds for use of his spinning disk confocal microscope. We thank Richard Poirier, Elena Savidov, Hanna Kroliczak and Dwayne Weber for technical help, and Dr. Patrick Lusk, Robert Scott and members of the Rachubinski laboratory for helpful discussions.

This work was supported by grant MT-9208 from the Canadian Institutes of Health Research (CIHR) to R.A.R. R.A.R. holds the Canada Research Chair in Cell Biology and is an International Research Scholar of the Howard Hughes Medical Institute. G.A.E. holds a New Investigator award from the CIHR and is a Scholar of the Alberta Heritage Foundation for Medical Research (AHFMR). M.F. is the recipient of an AHFMR Studentship.

Received: December 2, 2005
Revised: March 17, 2006
Accepted: April 6, 2006
Published: May 8, 2006

References

Adames, N.R., Oberle, J.R., and Cooper, J.A. (2001). The surveillance mechanism of the spindle position checkpoint in yeast. J. Cell Biol. *153*, 159–168.

Boldogh, I.R., Ramcharan, S.L., Yang, H.-C., and Pon, L.A. (2004). A type V myosin (Myo2p) and a Rab-like G-protein (Ypt11p) are required for retention of newly inherited mitochondria in yeast cells during cell division. Mol. Biol. Cell *15*, 3994–4002.

Bretscher, A. (2003). Polarized growth and organelle segregation in yeast: the tracks, motors, and receptors. J. Cell Biol. *160*, 811–816.

Catlett, N.L., Duex, J.E., Tang, F., and Weisman, L.S. (2000). Two distinct regions in a yeast myosin-V tail domain are required for the movement of different cargoes. J. Cell Biol. *150*, 513–526.

Estrada, P., Kim, J., Coleman, J., Walker, L., Dunn, B., Takizawa, P., Novick, P., and Ferro-Novick, S. (2003). Myo4p and She3p are required for cortical ER inheritance in *Saccharomyces cerevisiae*. J. Cell Biol. *163*, 1255–1266.

Fagarasanu, M., Fagarasanu, A., Tam, Y.Y.C., Aitchison, J.D., and Rachubinski, R.A. (2005). Inp1p is a peroxisomal membrane protein required for peroxisome inheritance in *Saccharomyces cerevisiae*. J. Cell Biol. *169*, 765–775.

Govindan, B., Bowser, R., and Novick, P. (1995). The role of Myo2p, a yeast class V myosin, in vesicular transport. J. Cell Biol. *128*, 1055–1068.

Hammond, A.T., and Glick, B.S. (2000). Raising the speed limits for 4D fluorescence microscopy. Traffic *1*, 935–940.

Hill, K.L., Catlett, N.L., and Weisman, L.S. (1996). Actin and myosin function in directed vacuole movement during cell division in *Saccharomyces cerevisiae*. J. Cell Biol. *135*, 1535–1549.

Hoepfner, D., van den Berg, M., Philippsen, P., Tabak, H.F., and Hettema, E.H. (2001). A role for Vps1p, actin, and the Myo2p motor in peroxisome abundance and inheritance in *Saccharomyces cerevisiae*. J. Cell Biol. *155*, 979–990.

Huh, W.-K., Falvo, J.V., Gerke, L.C., Carroll, A.S., Howson, R.W., Weissman, J.S., and O'Shea, E.K. (2003). Global analysis of protein localization in budding yeast. Nature *425*, 686–691.

Hwang, E., Kusch, J., Barral, Y., and Huffaker, T.C. (2003). Spindle orientation in *Saccharomyces cerevisiae* depends on the transport of microtubule ends along polarized actin cables. J. Cell Biol. *161*, 483–488.

Ishikawa, K., Catlett, N.L., Novak, J.L., Tang, F., Nau, J.J., and Weisman, L.S. (2003). Identification of an organelle-specific myosin V receptor. J. Cell Biol. *160*, 887–897.

Ito, T., Chiba, T., Ozawa, R., Yoshida, M., Hattori, M., and Sakaki, Y. (2001). A comprehensive two-hybrid analysis to explore the yeast protein interactome. Proc. Natl. Acad. Sci. USA *98*, 4569–4574.

Itoh, T., Toh-e, A., and Matsui, Y. (2004). Mmr1p is a mitochondrial factor for Myo2p-dependent inheritance of mitochondria in the budding yeast. EMBO J. *23*, 2520–2530.

Lee, L., Tirnauer, J.S., Li, J., Schuyler, S.C., Liu, J.Y., and Pellman, D. (2000). Positioning of the mitotic spindle by a cortical-microtubule capture mechanism. Science *287*, 2260–2262.

Liakopoulos, D., Kusch, J., Grava, S., Vogel, J., and Barral, Y. (2003). Asymmetric loading of Kar9 onto spindle poles and microtubules ensures proper spindle alignment. Cell *112*, 561–574.

Nagashima, K., Torii, S., Yi, Z., Igarashi, M., Okamoto, K., Takeuchi, T., and Izumi, T. (2002). Melanophilin directly links Rab27a and myosin Va through its distinct coiled-coil regions. FEBS Lett. *517*, 233–238.

Pastural, E., Barrat, F.J., Dufourcq-Lagelouse, R., Certain, S., Sanal, O., Jabado, N., Seger, R., Griscelli, C., Fischer, A., and de Saint Basile, G. (1997). Griscelli disease maps to chromosome 15q21 and is associated with mutations in the myosin-Va gene. Nat. Genet. *16*, 289–292.

Pruyne, D., Legesse-Miller, A., Gao, L., Dong, Y., and Bretscher, A. (2004). Mechanisms of polarized growth and organelle segregation in yeast. Annu. Rev. Cell Dev. Biol. *20*, 559–591.

Reck-Peterson, S.L., Provance, D.W., Jr., Mooseker, M.S., and Mercer, J.A. (2000). Class V myosins. Biochim. Biophys. Acta *1496*, 36–51.

Rief, M., Rock, R.S., Mehta, A.D., Mooseker, M.S., Cheney, R.E., and Spudich, J.A. (2000). Myosin-V stepping kinetics: a molecular model for processivity. Proc. Natl. Acad. Sci. USA *97*, 9357–9359.

Rossanese, O.W., and Glick, B.S. (2001). Deconstructing Golgi inheritance. Traffic *2*, 589–596.

Rossanese, O.W., Reinke, C.A., Bevis, B.J., Hammond, A.T., Sears, I.B., O'Connor, J., and Glick, B.S. (2001). A role for actin, Cdc1p, and Myo2p in the inheritance of late Golgi elements in *Saccharomyces cerevisiae*. J. Cell Biol. *153*, 47–62.

Schliebs, W., and Kunau, W.H. (2004). Peroxisome membrane biogenesis: the stage is set. Curr. Biol. *14*, R397–R399.

Schott, D., Ho, J., Pruyne, D., and Bretscher, A. (1999). The COOH-terminal domain of Myo2, a yeast myosin V, has a direct role in secretory vesicle targeting. J. Cell Biol. *147*, 791–807.

Schott, D.H., Collins, R.N., and Bretscher, A. (2002). Secretory vesicle transport velocity in living cells depends on the myosin-V lever arm length. J. Cell Biol. *156*, 35–39.

Seabra, M.C., and Coudrier, E. (2004). Rab GTPases and myosin motors in organelle motility. Traffic *5*, 393–399.

Shepard, K.A., Gerber, A.P., Jambhekar, A., Takizawa, P.A., Brown, P.O., Herschlag, D., DeRisi, J.L., and Vale, R.D. (2003). Widespread cytoplasmic mRNA transport in yeast: identification of 22 bud-localized transcripts using DNA microarray analysis. Proc. Natl. Acad. Sci. USA *100*, 11429–11434.

Spellman, P.T., Sherlock, G., Zhang, M.Q., Iyer, V.R., Anders, K., Eisen, M.B., Brown, P.O., Botstein, D., and Futcher, B. (1998). Comprehensive identification of cell cycle-regulated genes of the yeast *Saccharomyces cerevisiae* by microarray hybridization. Mol. Biol. Cell *9*, 3273–3297.

Tang, F., Kauffman, E.J., Novack, J.L., Nau, J.J., Catlett, N.L., and Weisman, L.S. (2003). Regulated degradation of a class V myosin receptor directs movement of the yeast vacuole. Nature *422*, 87–92.

Warren, G., and Wickner, W. (1996). Organelle inheritance. Cell *84*, 395–400.

Weisman, L.S. (2003). Yeast vacuole inheritance and dynamics. Annu. Rev. Genet. *37*, 435–460.

Wu, X., Jung, G., and Hammer, J.A., III. (2000). Functions of unconventional myosins. Curr. Opin. Cell Biol. *12*, 42–51.

Wu, X.S., Rao, K., Zhang, H., Wang, F., Sellers, J.R., Matesic, L.E., Copeland, N.G., Jenkins, N.A., and Hammer, J.A., 3rd. (2002). Identification of an organelle receptor for myosin-Va. Nat. Cell Biol. *4*, 271–278.

Yin, H., Pruyne, D., Huffaker, T.C., and Bretscher, A. (2000). Myosin V orientates the mitotic spindle in yeast. Nature *406*, 1013–1015.